2. Investigations for Low Prandtl Fluid

2.1 Numerical Simulation of Three Dimensional Oscillatory Flow in Half-Zone Bridges of Low Pr Fluids

Nobuyuki Imaishi

Kyushu University

NUMERICAL SIMULATION OF THREE DIMENSIONAL OSCILLATORY FLOW IN HALF-ZONE BRIDGES OF LOW Pr FLUIDS

Nobuyuki Imaishi*, Shouichi Yasuhiro* and Shinichi Yoda**

*Institute of Advanced Material Study, Kyushu University, Kasuga, 815-8580
**NASDA, Sengen 2-1-1, Tsukuba 305-8505

Several sets of numerical simulations were conducted to give realistic understandings of oscillatory Marangoni convection in half-zone liquid bridges of low Prandtl number fluid with various aspect ratios (from 0.6 to 2.2). Special emphasis was placed on the effects of the less-conductive supporting rods on the transition from axisymmetric steady flow to three dimensional steady and also to oscillatory three dimensional flow. The new simulation results revealed that the conductive heat transfer through the small gaps (1mm in total) between the melt/rod interface and the temperature measuring points causes significant temperature drop which provide with serious error in estimating Marangoni numbers. This conductive temperature drop is the major reason of the discrepancy between the numerical results in preceding years and the experimental results obtained in NASDA. The effect of the finite conductivity of the rods causes additional effect through the non-uniform temperature distributions on the melt/rod interface. This effect is not negligible but yet minor.

Keywords: Marangoni flow, Oscillatory flow, Critical Marangoni number, Low Pr fluid, Flow mode, conductive temperature drop

1. INTRODUCTION

Marangoni convection in a half-zone liquid bridge of length L and radius a confined between two differentially heated solid rods has become over the years a typical model for the study of thermocapillary flows and their stability. The stability of thermocapillary flow in non-isothermal liquid bridges with cylindrical free surface has been intensely investigated. These studies are stimulated by the experimental facts that flow instabilities in floating zones cause striations in crystals grown in microgravity condition. It is well known that the flow exhibits axisymmetric and steady roll cell structure under small temperature difference (ΔT) between the two disks and that it becomes unstable and a three-dimensional thermocapillary flow arises when the applied temperature difference exceeds a certain threshold value. On this subject, there have been many experimental works, theoretical studies by means of the linear stability analyses and non-linear numerical simulations. Most of those experimental works, however, have been extended for high Prandtl number fluids. Less works have been reported for low Prandtl number fluids, since it is very difficult to conduct well-controlled experiments with small Prandtl number fluids (mostly liquid metals) due to opacity, reactivity and high melting temperatures. On the other hand, numerical simulations have been conducted for thermocapillary flow in half-zone liquid bridges of various Prandtl numbers. Linear stability analyses (Neitzel et al.[1], Kuhlmann and Rath [2], Wanschura et al. [3], Chen et al. [4], Chen and Hu [5], Chen et al. [6]) have confirmed that for high Prandtl numbers the instability is oscillatory (Hopf bifurcation) whereas for low Prandtl numbers the

instability breaks the spatial axisymmetry (but the flow regime is still steady) prior to the onset of time dependent flow field. Recently, Levenstam et al.[7] studied the flow transitions in a half-zone at intermediate Prandtl numbers (0.05 – 1) using both linear stability analysis and numerical simulations. By means of direct numerical simulation techniques, Rupp et al. [8], Levenstan and Amberg [9] and Leypoldt et al. [10] confirmed that for low Prandtl number fluids, the first bifurcation is stationary i.e., the supercritical three-dimensional state is steady, and that the flow becomes oscillatory only when the temperature difference is further increased. These works had been conducted on limited range of the aspect ratios (As=L/a), mostly As=1.0 and 1.2.

In proceding years, we have conducted series of numerical simulations of Marangoni convection in half-zone liquid bridges of low Prandtl number fluids [11-18]. Part of these critical Reynolds numbers (or the critical Marangoni numbers) showed good agreements with those reported values by linear stability analysis [3,4] and other numerical simulations [9,10]. As was reported last year, our numerical simulations helped understand the structures of flow and temperature fields of 3-D steady flow and also types of oscillatory flows. We showed the first and the second critical Reynolds numbers as a function of aspect ratio and the Prandtl number. Our results indicate that the critical temperature difference (ΔTc) to initiate the oscillatory flow in liquid bridge of low Prandtl fluid increases as the aspect ratio decreases and shows maximum value at As=1.2. This trend was first reported by us but has never been confirmed experimentally. However, very few experimental reports are available on the flow instability in half zone liquid bridges of semiconductor materials [19-26] and molten tin [27-30]. These authors reported the existence of the oscillatory thermocapillary flows through their observations of the surface temperature oscillations, vibration of liquid bridge surface, and non-axisymmetric trajectories of tracer particles. The research group at NASDA succeeded to detect the second flow transitions by using a small liquid bridges of molten tin [27-30]. Their experimental results showed that ΔT_c tends to increase with decreasing aspect ratio. The results are qualitatively coincides with the aspect ratio dependency of our numerical results in large aspect ratio region. However, the experimentally determined critical Marangoni numbers (or the critical temperature differences between two rods measured by two thermocouples each of which is located in the iron rod only 0.5mm apart from each melt/rod interface) were as large as twice or more of our predictions, as shown in **Fig.1**. These discrepancies were pointed out in the last annual report [16], and left to be solved in the FY2001.

From a thermal engineer's point of view, the measured temperature differences do not represent the temperature difference which drives the thermocapillary flow, since there should be a considerable temperature drop in the supporting rod (made of iron) whose thermal conductivity is much smaller than that of molten tin. The smaller thermal conductivity of the supporting rods also originates non-uniform temperature distributions on the melt/rod interface. The two dimensional temperature distribution on the melt/rod interface may cause extra effects on the flow patterns and flow transitions. These effects of non-isothermal boundary conditions on the flow transitions have never been properly evalutaed by numerical simulations. The aim of our research in FY2001 is development of a new mathematical model and numerical codes, which can include the conductive heat transfer in the supporting rods and also the radiative heat loss from their surfaces. By running the codes, simulations predict the realistic stability limits at different aspect ratios under various imposed temperature differences. The results must be subjected to a quantitative comparison with the experimental results obtained by NASDA's group.

2. MODEL FORMULATIONS

In order to evaluate the effect of thermal resistance in the supporting solid rods extending both sides of the liquid bridge, cylindrical solid rods are added to a standard model of half-zone liquid bridge, as shown in **Fig. 2**. The origin of the z axis is located at the center of the lower melt/rod interface. The length of the liquid bridge is $a\times As$, the length of each rod is $a\times As_r$. The liquid surface is assumed non-deformable and cylindrical. This shape is true under microgravity condition. There acts the Marangoni effect on the liquid surface. Radiative heat loss from surfaces is also included. Fundamental equations are expressed as follows.

In the liquid bridge:

$$\frac{U}{R}+\frac{\partial U}{\partial R}+\frac{1}{R}\frac{\partial V}{\partial \theta}+\frac{\partial W}{\partial Z}=0$$

$$\frac{\partial U}{\partial \tau}+U\frac{\partial U}{\partial R}+\frac{V}{R}\frac{\partial U}{\partial \theta}-\frac{V^2}{R}+W\frac{\partial U}{\partial Z}=-\frac{\partial P}{\partial R}+\frac{\partial}{\partial R}\left\{\frac{1}{R}\frac{\partial(RU)}{\partial R}\right\}+\frac{1}{R^2}\frac{\partial^2 U}{\partial \theta^2}-\frac{2}{R^2}\frac{\partial U}{\partial \theta}+\frac{\partial^2 U}{\partial Z^2}$$

$$\frac{\partial V}{\partial \tau}+U\frac{\partial V}{\partial R}+\frac{V}{R}\frac{\partial V}{\partial \theta}+\frac{UV}{R}+W\frac{\partial V}{\partial Z}=-\frac{1}{R}\frac{\partial P}{\partial \theta}+\frac{\partial}{\partial R}\left\{\frac{1}{R}\frac{\partial(RV)}{\partial R}\right\}+\frac{1}{R^2}\frac{\partial^2 V}{\partial \theta^2}+\frac{2}{R^2}\frac{\partial V}{\partial \theta}+\frac{\partial^2 V}{\partial Z^2}$$

$$\frac{\partial W}{\partial \tau}+U\frac{\partial W}{\partial R}+\frac{V}{R}\frac{\partial W}{\partial \theta}+W\frac{\partial W}{\partial Z}=-\frac{\partial P}{\partial Z}+\frac{1}{R}\frac{\partial}{\partial R}\left(R\frac{\partial W}{\partial R}\right)+\frac{1}{R^2}\frac{\partial^2 W}{\partial \theta^2}+\frac{\partial^2 W}{\partial Z^2}+Gr\Theta$$

$$\mathrm{Pr}\left(\frac{\partial \Theta}{\partial \tau}+U\frac{\partial \Theta}{\partial R}+\frac{V}{R}\frac{\partial \Theta}{\partial \theta}+W\frac{\partial \Theta}{\partial Z}\right)=\frac{1}{R}\frac{\partial}{\partial R}\left(R\frac{\partial \Theta}{\partial R}\right)+\frac{1}{R^2}\frac{\partial^2 \Theta}{\partial \theta^2}+\frac{\partial^2 \Theta}{\partial Z^2}$$

In the solid rods,

$$\mathrm{Pr}\frac{\partial \Theta}{\partial \tau}=\alpha_{m/r}\left\{\frac{1}{R}\frac{\partial}{\partial R}\left(R\frac{\partial \Theta}{\partial R}\right)+\frac{1}{R^2}\frac{\partial^2 \Theta}{\partial \theta^2}+\frac{\partial^2 \Theta}{\partial Z^2}\right\}$$

Initial conditions: $U=V=W=0,\ \Theta=0$

Boundary conditions:

At both ends of the solid rods (Z=-As_r and Z=As+As_r):

$\Theta_{(R,\,\theta,\,-Asr)}$= +0.5, $\Theta_{(R,\,\theta,\,As+Asr)}$= -0.5

At the surface of the liquid bridge (R=1):

$$U=0,\quad \frac{\partial W}{\partial R}=\mathrm{Re}_T\frac{\partial \Theta}{\partial Z},\quad \frac{\partial}{\partial R}\left(\frac{V}{R}\right)=\mathrm{Re}_T\frac{1}{R}\frac{\partial \Theta}{\partial \theta}$$

$$\frac{\partial \Theta}{\partial R}=Bi^*\left\{\Theta+\frac{T_0}{\Delta T_T}-\frac{T_{amb}}{\Delta T_T}\right\}$$

At the surface of the rods (R=1):

$$\frac{\partial \Theta}{\partial R}=\frac{Bi^*}{\lambda_{r/m}}\left\{\Theta+\frac{T_0}{\Delta T_T}-\frac{T_{amb}}{\Delta T_T}\right\}$$

At the upper melt/rod interface (Z=As)

$$U=V=W=0,\quad \frac{\partial \Theta}{\partial Z}=\lambda_{r/m}\frac{\partial \Theta}{\partial Z}\Big|_{in\ rod}$$

At the lower melt/rod interface (Z=0)

$$U = V = W = 0, \quad \frac{\partial \Theta}{\partial Z} = \lambda_{r/m} \frac{\partial \Theta}{\partial Z}\Big| \ in\ rod$$

The non-dimensional parameters are the Prandtl number, Reynolds number, Biot number, as defined as follows, respectively. Radiation heat loss is evaluated by means of the Biot number.

$$Pr = \frac{\nu}{\alpha} = \frac{C_p \cdot \mu}{\lambda}$$

$$Re_T = -\frac{\partial \sigma_T}{\partial T} \Delta T_T a \Big/ (\mu \nu)$$

$$Bi^* = \frac{\varepsilon \sigma a}{\lambda_m} \Delta T_T^{\,3} \left\{ \left(\Theta + \frac{T_0}{\Delta T_T} \right)^2 + \left(\frac{T_{amb}}{\Delta T_T} \right)^2 \right\} \left\{ \Theta + \frac{T_o}{\Delta T_T} + \frac{T_{amb}}{\Delta T_T} \right\}$$

respectively. The Marangoni number is defined as Ma_T=$Re_T Pr$. The non-dimensional variables are defined as; $\{R, Z\}$= $\{r/a, z/a\}$, $P = pa^2/(\nu\mu)$, $U = ua/\nu$,$\Theta = (T\text{-}T_0)/\Delta T_T$, $\tau = t\nu/a^2$, where $T_0 = (T_h+T_c)/2$, $\alpha = \lambda/c_p \rho$, u: velocity, p: pressure, c_p: heat capacity, ρ: density, λ: thermal conductivity, μ: viscosity, ν: kinematic viscosity, σ: the Boltzman constant, $\alpha_{r/m} = \alpha_r / \alpha_m$, $\lambda_{r/m} = \lambda_r / \lambda_m$ and ΔT_T=(T_h-T_c).

It should be noted that the ΔT_T is the over all temperature difference imposed between the top and the bottom of the solid rods and it does not represent the temperature difference which drives the thermocapillary flow on the melt surface. The effective temperature difference acting on the liquid bridge and the temperature difference between the thermocouples in NASDA's experimental apparatus will be defined in the later part of this report.

3. NUMERICAL METHOD

These equations are discretized by a finite difference method with a modified central difference treatment for the convective terms [31] and non-uniform staggered grids. Non-uniform grids were adopted to increase the resolution. The radial velocities on the central axis were calculated by means of the method of Ozoe et al. [32]. A fully implicit code was developed this year using the Bi-CGSTAB (Bi-Conjugate Gradient STABility) method of Fujino et al. [33], combined with a specially coded matrix conditioner. This code provides very fast calculation, however, works only on the super computer. The code was validated by comparing the results with our previous numerical simulations run by different codes. The new code provides results with indistinguishable difference from the previous results. In this work, we did not give 3-D disturbances. But numerical disturbances grew up automatically. These numerical disturbances incubate 3-D disturbances automatically and they start growth with time if a super critical temperature difference is imposed. A two dimensional (2D) simulation code with the same scheme and 2D grids was run in order to obtain a 2D solutions under the same conditions. **Fig.3** shows one of the grids used for 2-D simulations. For three dimensional cases, similar grids were generated on each of n vertical cross sections on every $\Delta\theta = \pi/n$. In the present simulations, n= 20-24 was chosen for various aspect ratios. The thermophysical properties and geometric parameters are listed in **Table 1**.

4. RESULTS

4.1 Flow and temperature fields for As=2.0

First, a series of simulations for tin liquid bridge with a fixed aspect ratio of As=2 with different imposed over-all temperature differences as shown in **Table 2**. In these cases, we assumed g=0 (zero-gravity condition).

Case 1: ΔT_T=4.37K (Ma_T=30)

In this case the thermocapillary flow in the liquid bridge is axisymmetric and steady. At τ=0, the bottom plate of the lower rod is subjected to an instantaneous temperature rise from Θ=-0.5 to up to Θ=+0.5 (real temperature rise in this case is 4.37K). The lower rod is heated up via unsteady heat conduction and the liquid bridge and the upper rod are heated up. As the liquid bridge is subjected to a non-isothermal condition, thermocapillary flow starts as shown in **Fig.4**. As time passes in the early stage, the surface velocity increases very quickly. But with this small ΔT_T the induced flow is steady and axisymmetric. After time τ=0.2, the surface velocity is maintained at a constant value, indicating that the effective temperature difference between the lower and the upper melt/rod interfaces and the flow has reached their final conditions. However, the lower figure indicates that the temperature level in the liquid bridge is still rising until τ=0.65. Temperature and velocity distributions at the steady state are shown in **Fig. 5**. The isotherms are drawn at every $\Delta\Theta$=0.02 on the vertical cross section and $\Delta\Theta$=0.001 on the horizontal cut planes. The horizontal cut planes at the cold and the hot end of the liquid bridge show small coaxial non-uniformity of temperature (yet less than 0.013K). The isotherms in the melt are horizontal and parallel. Heat transfer in the melt is practically controlled by the conduction. The effective temperature difference between the upper and the lower ends of the liquid bridge is 0.96K and the effective Marangoni number is Ma=6.6.

Case 2: ΔT_T=10.93K (Ma_T=75)

The simulated results are shown in **Fig.6** and **Fig.7**. In the early stage, an axisymmetric thermocapillary flow field develops. This axisymmetric flow is unstable against a three dimensional disturbance. From an early stage, small 3-D disturbance (see Fig.6, local absolute azimuthal velocity ($|U_\theta|$) on the melt surface) grows exponentially with time and becomes distinguishable after τ=0.65. Finally, a steady three dimensional flow and temperature field comes out as shown in Fig.7. The isotherms are drawn at every $\Delta\Theta$=0.02 on the vertical cross section and $\Delta\Theta$=0.002 on the horizontal cut planes. The horizontal cut planes at the cold and the hot end of the liquid bridge show small two-dimensional temperature (yet less than 0.66K). The shape of the isotherms in horizontal cuts look like a horse-shoe, suggesting that the 3-D flow has an azimuthal wave number of m=1. The isotherms in the melt are almost parallel but distinguishably and three dimensionally deformed. 3-D convective transfer in the melt takes important role in the 3-D flow. The effective temperature difference between the upper and the lower ends of the liquid bridge is 2.37K during the pseudo axisymmetric flow period. But it increases up to 2.38K at the 3-D steady flow. The flow transition from an axisymmetric to a 3-D steady flow is accompanied by a small (0.5%) reduction of the over-all heat transfer coefficient in the melt. The effective Marangoni number based on the averaged surface temperature difference $\Delta\overline{\Theta}$ is Ma=16.32.
The averaged surface temperature difference $\Delta\overline{\Theta}$ is defined as : $\Delta T = \Delta\overline{\Theta} \times \Delta T_T$ where $\Delta\overline{\Theta}$ is defined as:

$$\Delta\overline{\Theta} = \left\{ \int_0^{2\pi} \Theta_{(1,\theta,0)} \mathrm{d}\theta - \int_0^{2\pi} \Theta_{(1,\theta,As)} \mathrm{d}\theta \right\} / 2\pi .$$

Case 3: ΔT_T=17.48K (Ma_T=120)

The simulated results are shown in **Fig.8**. From the early stage, a 3-D disturbances are growing. For a very short period, a pseudo steady 2-D flow field appears ($0.1<\tau<0.2$) but

after at τ=0.16, a 3-D disturbance starts increasing its intensity. The exponential growth ends at around τ=0.25. At the last moment of the growth, an oscillatory disturbance is excited. However, the amplitude of this oscillation stays small and very slowly decreases with time. The final flow state should be a 3-D steady flow with m=1. $\Delta\overline{\Theta}$ is about 0.2156 at the fully developed stage. Then the effective Marangoni number is Ma=25.87. This value is slightly smaller than the second critical condition (Ma_2=25.93). This small sub-critical state is the cause of the slow decay of the accidentally excited oscillations.

Case 4: ΔT_T=18.94K (Ma_T=130)

The simulated results are shown in **Fig.9**. At τ=0.16 a 3-D disturbance starts its growth process. For a very short period, a pseudo steady 2-D flow field appears ($0.1<\tau<0.2$) but after τ=0.24, transition to a 3-D flow field occurs and an oscillatory disturbance is superposed on the basic 3-D flow and increases its amplitude exponentially with time. Finally the flow and temperature fields exhibit oscillations with yet small amplitudes. The non-uniformity of the interface temperature becomes larger than those in the previous case. The melt flow pattern is classified as a twisting type oscillation with m=1. $\Delta\overline{\Theta}$ is about 0.2152 during the fully developed oscillation. Then the effective Marangoni number is Ma=27.98.

Case 5: ΔT_T=20.40K (Ma_T=140)

The simulated results are shown in **Fig.10** and **11**. A transition to 3-D flow occurs at around τ=0.25. At the same time oscillatory disturbance increases its oscillation amplitudes. At this condition, oscillatory disturbances grow much faster and bigger and become easily detectable. Finally the flow and temperature fields exhibit oscillations with constant amplitudes and period as shown in Fig.10. The isotherms in Fig.11 are drawn at every $\Delta\Theta$=0.02 on the vertical cross section and $\Delta\Theta$=0.0025 on the horizontal cut planes.. The non-uniformity of the interface temperature becomes larger than those in the previous case. The melt flow pattern is classified as a twisting type oscillation with m=1. $\Delta\overline{\Theta}$ is about 0.2147. Then the effective Marangoni number is Ma=30.06.

Case 6: ΔT_T=26.23K (Ma_T=180)

The simulated results are shown in **Fig.12** and **13**. A transition to 3-D flow occurs at around τ=0.25. At the same time twisting type oscillatory disturbance of m=2 increases its oscillation amplitudes and soon become detectable. But after around τ=0.8, a transition of flow occurred accompanied by a significant decrease of $\Delta\Theta$ for a short time. After τ=1.15, a twisting type oscillatory flow with m=1 becomes dominant. Thereafter, oscillatory flow of m=1 is prevailing but the flow and temperature fields become unstable and the periods and amplitudes of disturbances are time dependent. $\Delta\overline{\Theta}$ is about 0.213 during the m=1 period. Then the effective Marangoni number is about Ma=38.34.

4.2 Critical Marangoni numbers for flow transitions in a liquid bridge of As=2.0

From these simulation results mentioned above, we can calculate the growth rate constant β of a 3-D steady or oscillatory disturbances. Thus determined β's are plotted as a function of the effective Reynolds number as shown **Fig.14** and **Fig.15** for the first transition and the second transition, respectively. In the plots, the results of our previous simulations which assumed isothermal melt/rod interfaces. Fig.14 indicates that the first critical Reynolds number is insensitive to the thermal conductivity of the supporting rods, i.e., isothermal case

predicted Re_{c1}=790.5 and the present results based on the effective ΔT gives 791.9. Deviation is less than 0.2%. This reflects the fact that at the first flow transition condition, heat flux through the liquid bridge is small and the melt/rod interface is practically isothermal even if the rod has smaller thermal conductivity than the melt. However, for the second critical Reynolds number, the small thermal conductivity of the rods causes a small increase of the critical Reynolds number. The isothermal case predicted the second critical condition as Re_{c2}= 2819, ω_{c2}=136.4 and the present result 2903, ω_{c2}=140.5. The deviation is yet less than 3%.

With this model, we evaluated the effect of radiative heat loss, from the surfaces of the melt and the rods, on the second critical Reynolds number and the critical oscillatory frequency. Under the radiative boundary conditions with ε=0.1 and T_{amb}=390K, the present model predicted the second critical conditions as follows.
If we assume the isothermal melt/rod interfaces: Re_{c2}=2828 and ω_{c2}=138.2.
If we assume two iron rods support the liquid bridge: Re_{c2}=2917.7 and ω_{c2}=141.4.

Thus the radiation heat loss provides small increase (by about 3.5%) of the second critical Reynolds number from the isothermal, adiabatic case in our previous result.

4.3 Effect of the finite thermal conductivity of the rods on the critical conditions in different aspect ratios

Similar set of simulations were conducted for a liquid bridge with As=1.4 and an adiabatic surface. The results predicted Re_{c2}=4783 and ω_{c2}=220.3. The isothermal boundary conditions at both melt/rod interface gives Re_{c2}=4628 and ω_{c2}=212.8 for Pr=0.01.

Thus, the radiation heat loss and the non-isothermal boundary conditions can not explain the large deviation between the experimental results and our simulation results shown in Fig.1.

4.4 Effect of the conduction in the rods.

The results of the preceding sections suggest that the critical Reynolds numbers are not sensitive to the small temperature non-uniformities on the both interfaces. Thus the very large deviations between the second critical Reynolds numbers predicted by the simulations and the experiments must be understood by different factors. The most plausible cause of these deviations
may be the differences between the effective temperature difference between the melt/rod interfaces (ΔT_1) and the temperature difference between the measuring point (ΔT_2). Although the vertical distance between the interface and the tip of the thermocouple (δ) is as small as 0.5mm, it should be noted that the heat flux in the liquid bridge of low Pr fluid tend to be large. Our previous simulation results predicted that as the aspect ratio decreases, the larger temperature difference is required to initiate oscillatory convection, for aspect ratios larger than 1.2. Thus, the heat flux must increase as the As decreases.
A very crude model predict the temperature drop in this small distance (δ) between the interface and the temperature measuring point. As shown in **Fig.16**, temperature difference between the interfaces is denoted as ΔT_1 and that between the two measuring points is denoted as ΔT_2. If we assume that the heat transfer in the melt is also governed by the heat conduction, following equations are easily derived.

$$q = \frac{\lambda_m}{L}\Delta T_1, \quad q = \frac{\lambda_r}{\delta}\Delta T_\delta, \quad and \quad \Delta T_2' \approx \Delta T_1 + 2\Delta T_\delta$$

where ΔT_δ is the temperature drop in the distance δ. Thus, the ratio of these two temperature differences is a function of the aspect ratio as;

$$\frac{\Delta T_2'}{\Delta T_1} = 1 + \left(\frac{2\delta}{a}\right)\left(\frac{\lambda_m}{\lambda_r}\right)\frac{1}{As} \quad .$$

The reported values of the second critical Marangoni number of NASDA's experiments were calculated based on the temperature difference between two thermocouples (ΔT_2). These values can't be expected to represent ΔT_1 but rather closer to this $\Delta T'_2$. Hereafter, we define a Marangoni number based on ΔT_2 and denote it as *Ma'*, i.e., $Ma' = (\Delta T_2 / \Delta T_1) Ma$.
Then, the second critical Marangoni numbers predicted by our simulations with isothermal boundary conditions on both end plates (indicated by the solid triangles in **Fig.17**) can be approximated by adopting this crude model as,

$$Ma' = \frac{\Delta T_2}{\Delta T_1} Ma \approx \left\{1 + \left(\frac{2\delta}{a}\right)\left(\frac{\lambda_m}{\lambda_r}\right)\frac{1}{As}\right\} Ma$$

This equation converts the Ma_{c2} of our previous work to Ma'_{c2} as indicated by the dotted line in Fig.17.

These approximated values are compared with the *Ma'* values based on the three dimensional simulations with the iron rods.
The temperature differences between two locations of thermocouples can be easily obtained from the simulations. Thus calculated values of Ma'_{c2} at As=2.0 and As=1.4 are also plotted in Fig.17. These points fall very close to the dotted line, indicating the crude model can be used as a first approximation to convert *Ma* to *Ma'* or vise versa.

As shown in Fig.17, the experimentally determined second critical Marangoni numbers based on the measured ΔT_2 show large scatters but most of them fall above the dotted line and the Ma_{c2} based on the present 3-D simulation results. The smallest value at each As suggest the dotted line gives a reasonable criteria for the incipience of the oscillatory Marangoni flow in the tin liquid bridges. That means, the second critical Marangoni numbers as a function of aspect ratio, first predicted by us via 3-D simulations is confirmed by the experiments using tin liquid bridges at NASDA. However, the scatters of the experimental results are very large and the reliability of those experimental results must be further evaluated critically.

5. Conclusion

2000 Annual Report of NASDA's Marangoni Convection Research Project reported our simulation results and NASDA's experimental results on the critical temperature difference to initiate the oscillatory flow in a small liquid bridge of molten tin. The experimental results of the critical temperature difference (ΔT_C) were larger than our simulation results by a factor of 2 to 3. In order to evaluate the true causes of these discrepancies, a new mathematical model was developed this year. The new model includes radiative heat loss and the supporting rods which has lower thermal conductivity than the liquid in the liquid bridge. The developed numerical codes were run using the same physical properties and geometrical parameters as those of the experimental set-ups of NASDA's experimental apparatus. The lower thermal

conductivity of the iron rods and the radiation heat loss from the liquid surface cause small increase of the second critical temperature difference (or the critical Reynolds number) compared with our previous results which assumed isothermal disks. The increases, however, are less than 3.5%. However, these simulation results and a thermal engineering analysis revealed the real cause of the discrepancy between our results and NASDA's experimental results. The spatial gap between the melt/rod interface and the temperature measuring point, as small as 0.5mm, create significant temperature drops and the measured ΔT_C did not represent the effective temperature difference which drived the thermocapillary flow. Heat flux in the rods and short liquid bridge of molten tin cause unexpectedly large temperature drops in the rods. The experimental results must be critically analyzed before being compared with theoretical predictions.

7. References

[1] G.P. Neitzel., K.T. Chang, D.F. Jancowski, H.D. Mittelmann, "Linear stability of thermocapillary convection in a model of the float-zone crystal-growth process", *Phys. Fluids* A 5, 108-114 (1992).

[2] Kuhlmann H.C., Rath H.J., (1993), "Hydrodinamic instabilities in cylindrical thermocapillary liquid bridges", *J.Fluid Mech.* , 247, 247-274

[3] M. Wanschura, V. Shevtsova, H.C. Kuhlmann, H.J. Rath, "Convective instability mechanism in thermocapillary liquid bridges", *Phys. Fluids*, **5**, (1995), 912-925

[4] G. Chen, A. Lizee, B. Roux, "Bifurcation analysis of the thermocapillary convection in cylindrical liquid bridges", *Journal of Crystal growth*, **180**, (1998), 238-647

[5] Q.S. Chen, W.R. Hu, "Influence of liquid bridge volume on instability of floating half-zone convection", *Int. J. Heat Mass Transfer,* 41, 825-837 (1998).

[6] Q.S. Chen, W.R. Hu, V. Prasad, "Effect of liquid bridge volume on the instability in small-Prandtl-number half zones", *Journal of Crystal growth*, **203**, (1999), 261-268

[7] M. Levenstam, G. Amberg, W. Christian,"Instabilities of thermocapillary convection in a half-zone at intermediate Prandtl numbers", *Physics of Fluids,* **13(4)**, (2001), 807-816.

[8] R. Rupp, G. Mueller, G. Neumann, "Three dimensional time dependent modeling of the Marangoni convection in zone melting configurations for GaAs", *Journal of Crystal growth*, **97**, (1989), 34-41

[9] M. Levenstam, G. Amberg, "Hydrodynamical instabilities of thermocapillary flow in a half-zone", *J. Fluid Mechanics*, **297**, (1995), 357 -372

[10] J. Leypoldt, H.C. Kuhlmann, H.J. Rath, "Three-dimensional numerical simulation fo thermocapillary flows in cylindrical liquid bridges", *J. Fluid Mech*, **414**, 285, (2000)

[11] N. Imaishi, S. Yasushiro, T. Sato, S. Yoda, "Three dimensional numerical simulation of oscillatory Marangoni flow in a half zone of low Pr fluids", Material Research in low gravity II, Vol 3792, 344-352 (SPIE The International Society for Optical Engineering), 19-21 July 1999, Denver, Colorado

[12] N. Imaishi, S. Yasushiro, T. Sato, S. Yoda, "Numerical simulation of three dimensional oscillatory flow in half zone bridges of low Pr fluid", Proceedings of the 4th JSME-KSME Thermal Engineering Conference - October 1-6, 2000, Kobe, Japan, 272-282

[13] S. Yasushiro, T. Sato, N. Imaishi, S.Yoda "Three dimensional Marangoni flow in liquid bridge of low Pr fluid", Space Forum, **6**, 39-47 (2000)

[14] N. Imaishi, S. Yasuhiro, S. Yoda, " Numerical simulation of three dimensional oscillatory in half-zone liquid bridge of low Pr fluids" in "NASDA Technical Memorandum, Marangoni Convection Modeling Research Annual Report of FY 1999",

NASDA-TMR-000006E, pp.159-178 (2000)
[15] N. Imaishi, "Role of the Marangoni effect on melt convection ", Abstract of the 3rd Int. Workshop on Modeling in Crystal Growth ,115-116 (Stony Brook, Oct. 19, 2000)
[16] N. Imaishi, S. Yasuhiro, S. Yoda, " Numerical simulation of three dimensional oscillatory in half-zone liquid bridge of low Pr fluids" in "NASDA Technical Memorandum, Marangoni Convection Modeling Research Annual Report of FY 2000", NASDA-TMR-010015E, pp.133-144 (2001)
[17] N. Imaishi, S.Yasuhiro, Y. Akiyama, S. Yoda," Three dimensional Marangoni flow in half-zone liquid bridge of low Pr fluid", *Journal of Crystal Growth*, **vol.230**: (1-2) pp.164-171 (2001)
[18] N. Imaishi, S.Yasuhiro, Y. Akiyama, S. Yoda, " Numerical simulation of 3-Dimensional Marangoni Flow in Liquid Bridge of Low Pr Fluids", *J. Jpn. Soc. Microgravity Appl.* (in Japanese), **18,** (2001) pp. 2-10.
[19] S. Nakamura, K. Kakimoto, T. Hibiya, (1995), "Convection visualization and temperature fluctuation measurement in a molten silicon column", Materials and fluids under low gravity (Springer), Proceedings of the IXth European Symposium on Gravity-Dependent Phenomena in Physical sciences Held at Berlin, Germany, 2-5 May 1995
[20] S. Nakamura, T. Hibiya, K. Kakimoto, N. Imaishi, S-i Nishizawa, A. Hirata, K. Mukai, S-i Yoda, T. S. Morita, "Temperature fluctuations of the Marangoni flow in a liquid bridge of molten silicon under microgravity on board the TR-I4 rocket", *Journal of Crystal Growth* ,**186**, 85, (1998).
[21] T. Hibiya, S. Nakamura, N. Imaishi, K. Mukai, K. Onuma, P. Dold, A. Croll, K-W Benz, S-i Yoda, "Marangoni flow of Si melt: microgravity experiments and perspective", J. Jpn. Soc. Microgravity Appl. Supplement, Proc. Joint 1st Pan-Pacific Basin Workshop and 4th Japan-China Workshop on Microgravity Sciences (1998).
[22] T. Azami, S. Nakamura, T. Hibiya, S. Nakamura, "The effect of oxygen on the temperature fluctuation of Marangoni convection in a molten silicon bridge" , *Journal of Crystal Growth,* **223**, pp.116-124, (2001).
[23] M. Sumiji, S. Nakamura, T. Azami, T. Hibiya, " Optical observeation of solid-melt interface fluctuation due to Marangoni flow in a silicon liquid bridge", *Journal of Crystal Growth,* **223**, pp. 503-511, (2001).
[24] T. Azami, S. Nakamura, T. Hibiya, " Observation of periodic thermocapillary flow in a molten silicon bridge by using non-contact temperature mesurements", *Journal of Crystal Growth*, **231**, pp. 82-88, (2001).
[25] M. Sumiji, S. Nakamura, T. Hibiya," Two-directional observation of solid-melt interface fluctuation induced Marangoni flow in a silicon liquid bridge", *Journal of Crystal Growth,* **235**, pp. 55-59, (2002).
[26] T. Azami, S. Nakamura, T. Hibiya, "Marangoni convection of molten silicon: Microgravity Experiments and Crystal Growth", *J. Jpn. Soc. Microgravity Appl.* (in Japanese), **18,** (2001), pp. 16-25.
[27] K. Takagi, M. Ohtaka, H. Natsui, T. Arai, S. Yoda, " Experimental study of thermocapillary flow in the half-zone liquid bridge of low Prandtl number fluid", in "NASDA Technical Memorandum, Marangoni Convection Modeling Research Annual Report of FY 1999", NASDA-TMR-000006E, pp.117-156, (2000)
[28] K. Takagi, M. Ohtaka, H. Natsui, T. Arai, S. Yoda, Z. Yuan, K. Mukai, S. Yasuhiro, N. Imaishi, " Experimental study on transition to oscillatory thermocapillary flow in a low Prandtl number liquid bridge", *Journal of Crystal Growth,* **233**, pp. 399-407, (2001).
[29] K. Takagi, M. Ohtaka, H. Natsui, T. Arai, S. Yoda, "Experimental study on transition to oscillatory thermocapillary flow in molten tin column", *J. Jpn. Soc. Microgravity Appl.*

(in Japanese), **18,** (2001), pp. 11-15.
[30] M. Ohtaka, K. Takagi, H. Natsui, T. Arai, S. Yoda, "Experimental study of thermocapillary flow in the half-zone liquid bridge of low Prandtl number fluid",in, "NASDA Technical Memorandum, Marangoni Convection Modeling Research Annual Report of FY 2000", NASDA-TMR-010015E, pp.147-180, (2000)
[31] T. Suzuki, and H. Kawamura, *J. Mech. Eng. Japan (in Japanese)*, **60**-578(B), 58 (1994)
[32] H. Ozoe and K. Toh, "Dopant concentration profile in a Czochralski flow of liquid metal in a vertical or a horizontal magnetic field", *J. Crystal Growth*, **130**, 645-656 (1993).
[33] S.Fujino, K. Miura, "An effective guideline for BiCGSTAB(L) method", RIMS, 2002. (in print)

Table 1 Thermophysical properties and geometric parameters.

			Molten Tin	Iron
Pr			0.009	-
Density	ρ	[kg/m3]	6793	7700
Thermal conductivity	λ	[W/mK]	35.44	20.0
Specific heat	Cp	[J/kgK]	242	460
Viscosity	μ	[kg/ms]	$1.318 \cdot 10^{-3}$	-
Temperature coefficient of surface tension	σ_T	[N/mK]	$-1.3 \cdot 10^{-4}$	-
Emissivity	ε	[-]	0.1	0.11(SKD11)
				0.16(SUS316)
Radius	a	[m]	$1.5 \cdot 10^{-3}$	
Length of the liquid bridge	L	[m]	$3.0 \cdot 10^{-3}$	
Total length		[m]	$9.0 \cdot 10^{-3}$	
Ambient temperature	T_{amb}	[K]	390	

Table 2 Overall temperature differences and Ma_T imposed for numerical simulation.

	ΔT_T [K]	Ma_T [-]
Case1	4.37	30
Case2	10.93	75
Case3	17.48	120
Case4	18.94	130
Case5	20.40	140
Case6	26.23	180

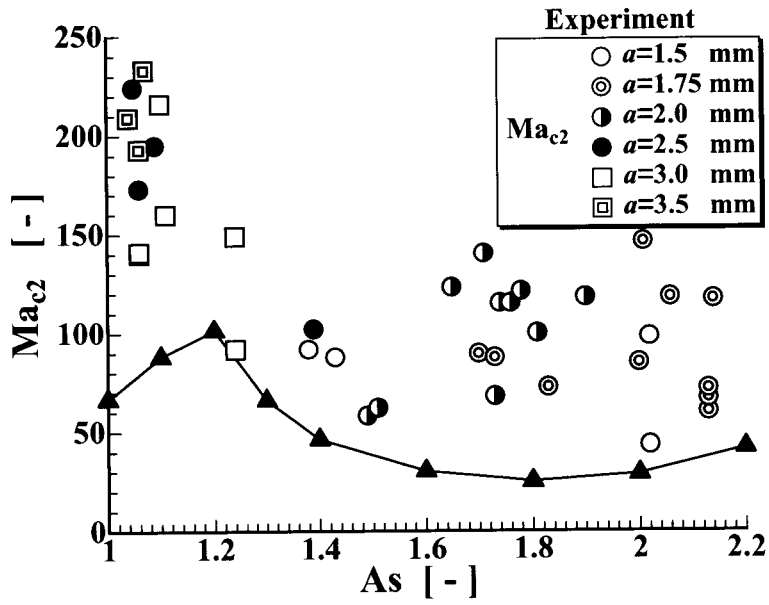

Fig. 1 Comparison of the experimentally determined Ma_{c2} and our simulation results for tin bridges as a function of aspect ratio.

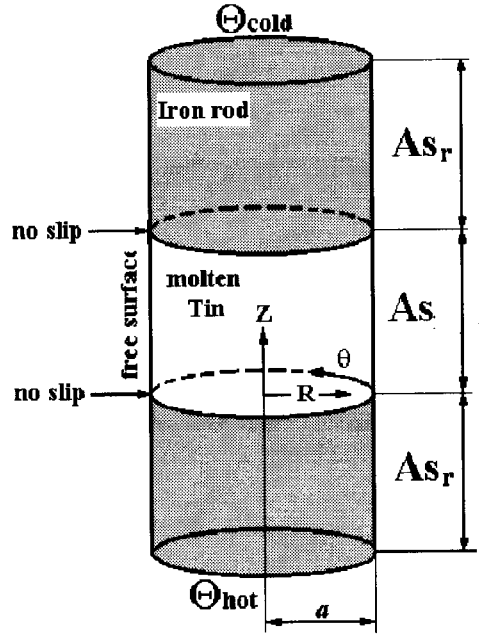

Fig. 2 Schematics of a liquid bridge with two supporting rods.

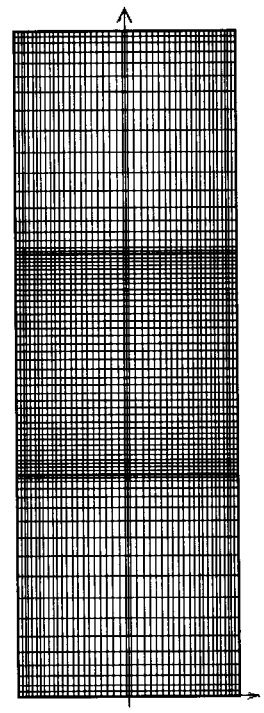

Fig. 3 One example of the grid used in the present simulations.

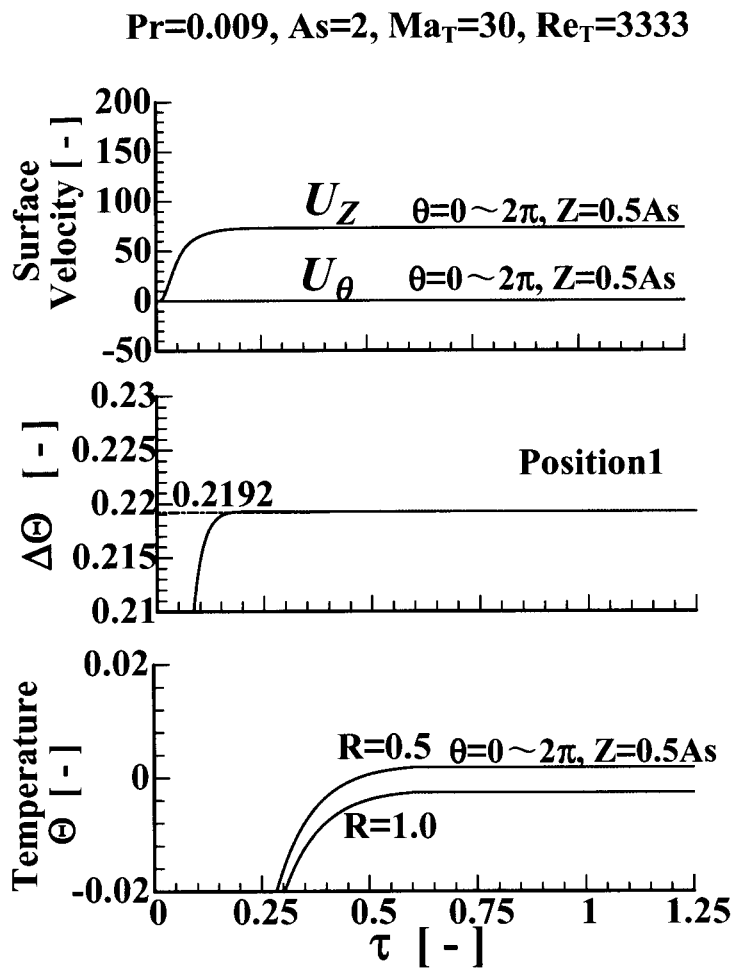

Fig.4 Time evoluton of a 3-D oscillatory Marangoni flow in a bridge of Pr=0.009, As=2, Ma_T=30, Re_T=3333 and ΔT_T=4.37K

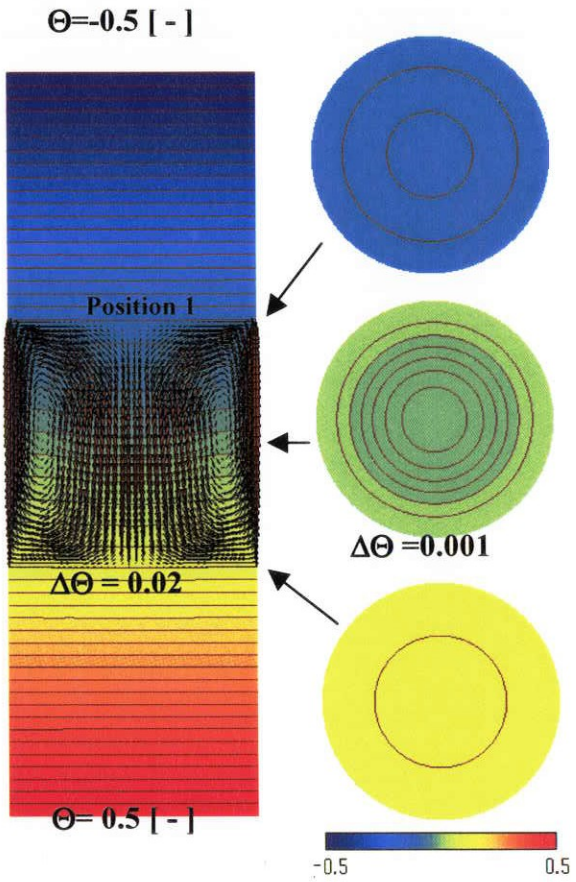

Fig. 5 Snapshots of velocity and temperature distributions in a vertical cut plane and horizontal cuts at Z= As_r , As_r+0.5As and As_r + As at axisymmetric steady stage of Pr=0.009, As=2, Ma_T=30, Re_T=3333 and ΔT_T=4.37K

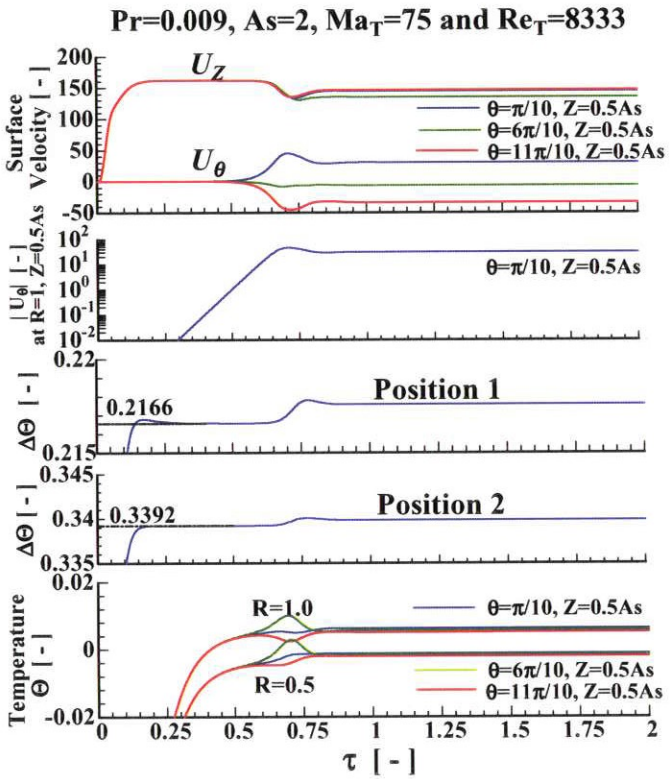

Fig. 6 Time evoluton of a 3-D oscillatory Marangoni flow in a bridge of Pr=0.009, As=2, Ma_T=75, Re_T=8333 and ΔT_T=10.93K

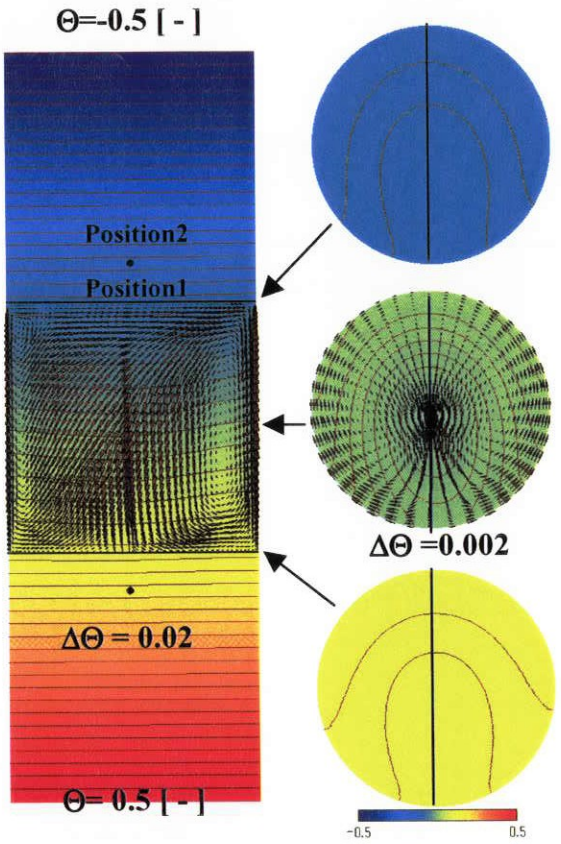

Fig. 7 Snapshots of velocity and temperature distributions in a vertical cut plane and on $Z=As_r$, $As_r+0.5As$ and As_r + As horizontal cut planes at finally 3D steady stage of Pr=0.009, As=2, Ma_T=75, Re_T=8333 and ΔT_T = 10.93K

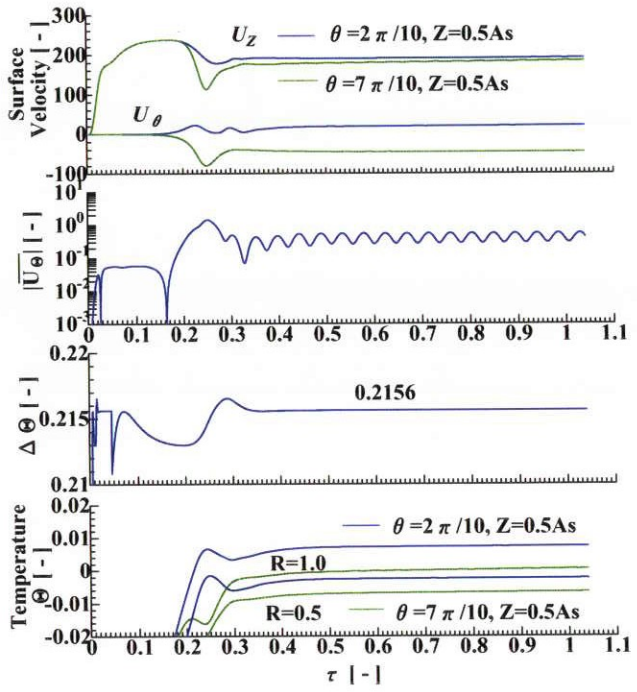

Fig.8 Time evoluton of a 3-D oscillatory Marangoni flow in a bridge of $\Delta T_T = 17.48$ K and Ma_T=120

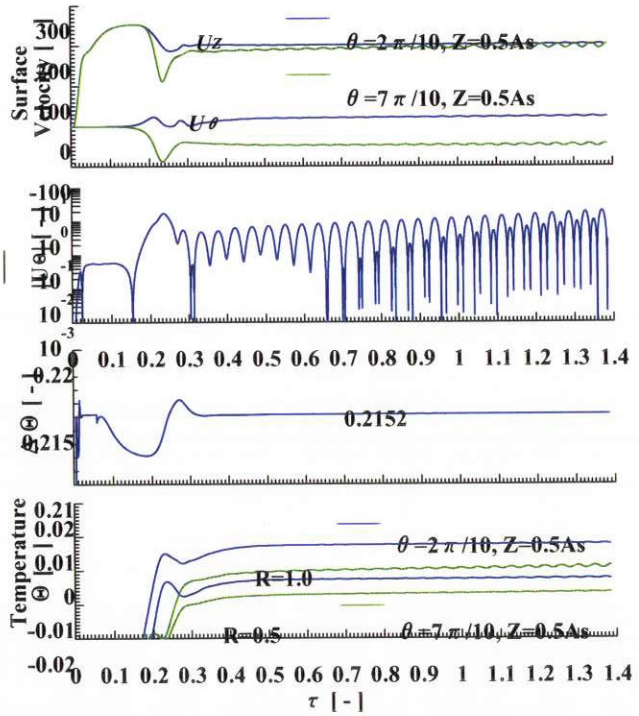

Fig. 9 Time evoluton of a 3-D oscillatory Marangoni flow in a bridge of ΔT_T=18.94K and Ma_T=130

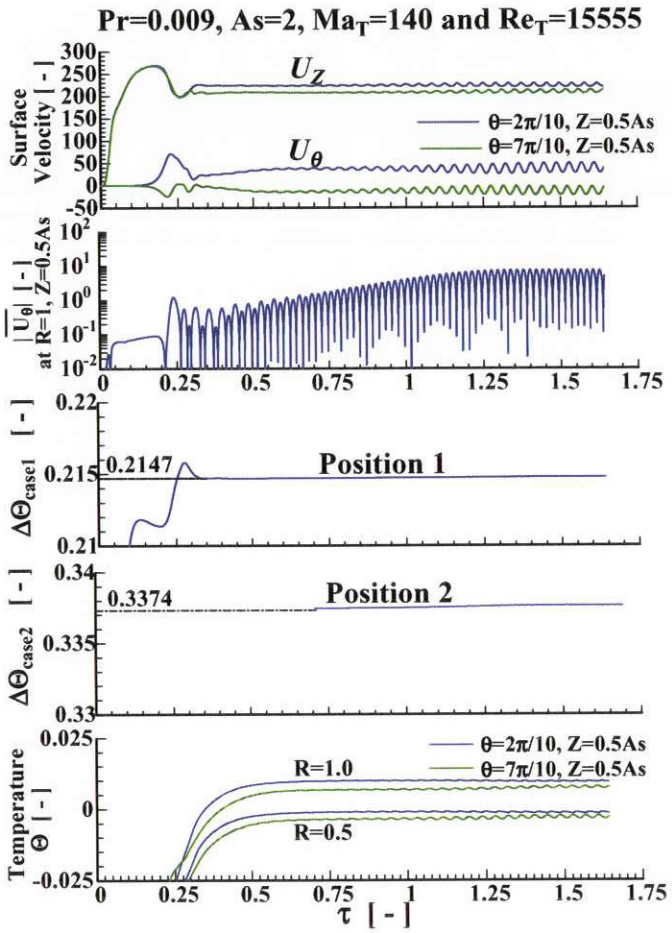

Fig.10 Time evoluton of a 3-D oscillatory Marangoni flow in a bridge of $\Delta T_T = 20.40$ K and $Ma_T = 140$

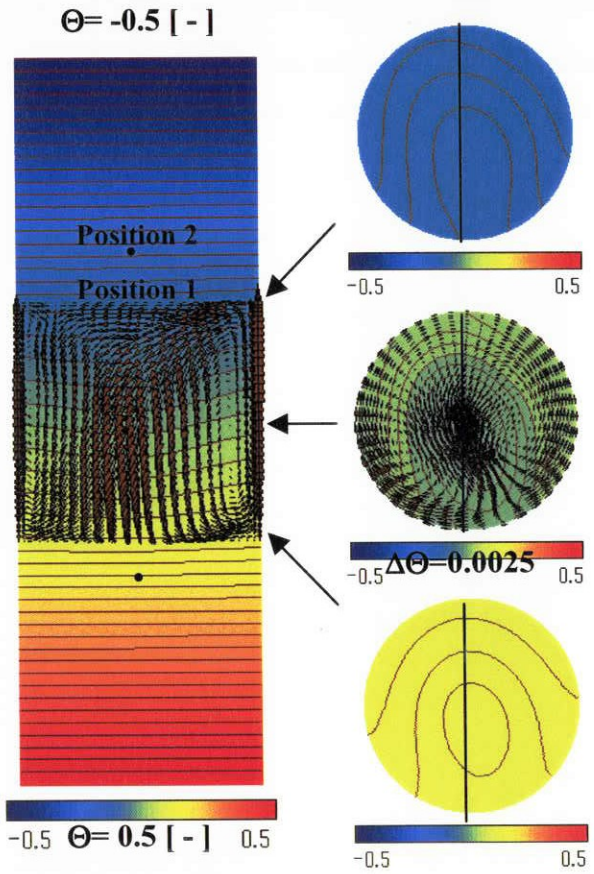

Fig. 11 Snapshots of velocity and temperature distributions in a vertical cut plane and on $Z=$ As_r, $As_r+0.5As$ and $As_r + As$ horizontal cut planes at finally 3D oscillatory stage of $\Delta T_T=$ 20.40 K and Ma_T=140.

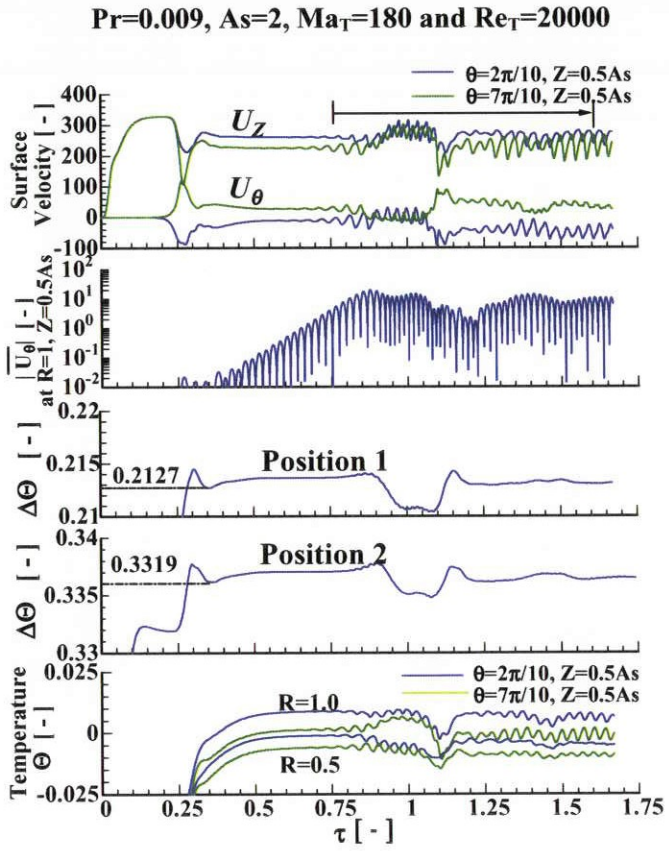

Fig.12 Time evoluton of a 3-D oscillatory Marangoni flow in a bridge of $\Delta T_T = 26.23$ K and $Ma_T = 180$.

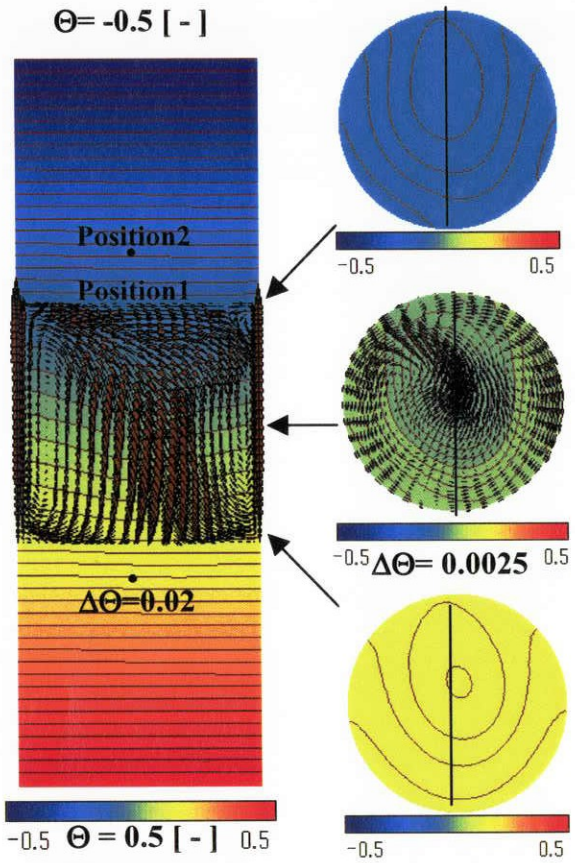

Fig.13 Snapshots of velocity and temperature distributions in a vertical cut plane and on Z= As_r , As_r+0.5As and As_r + As horizontal cut planes at finally 3D oscillatory stage of ΔT_T = 26.23 K and Ma_T=180.

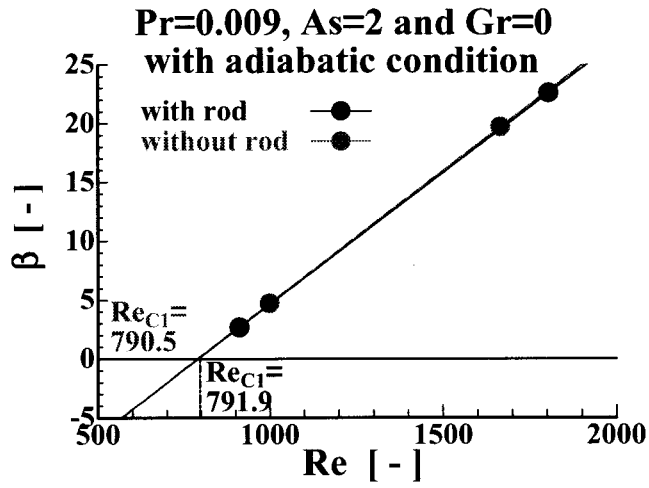

Fig.14 The first critical condition

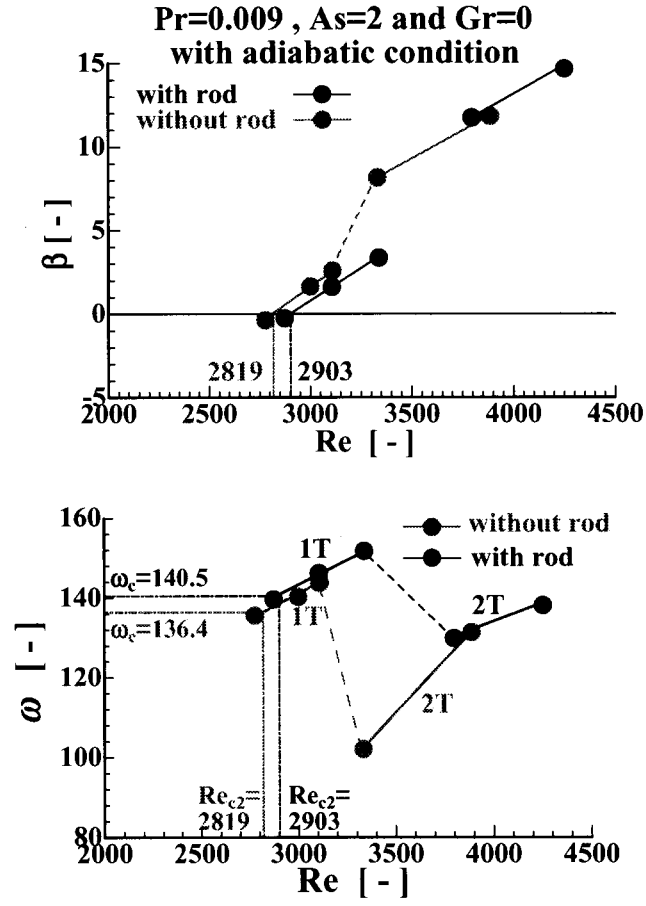

Fig.15 The second critical condition.

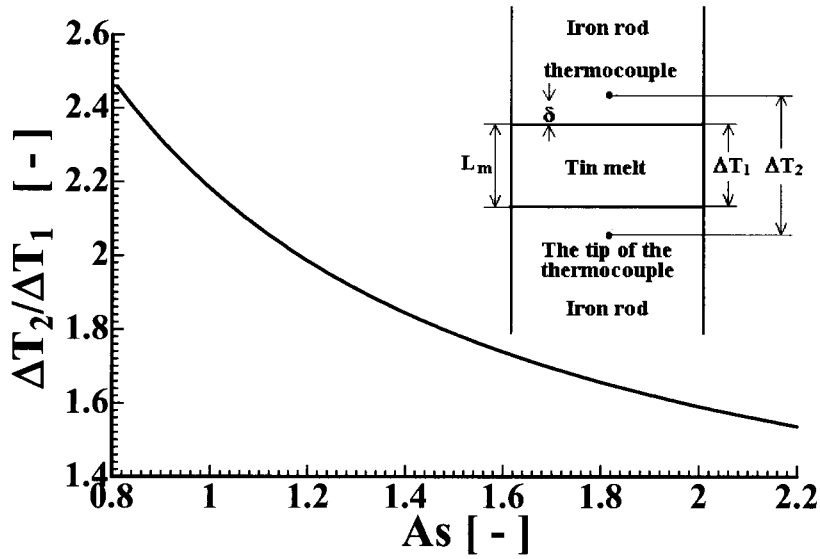

Fig.16 ΔT2/ΔT1 vs. As

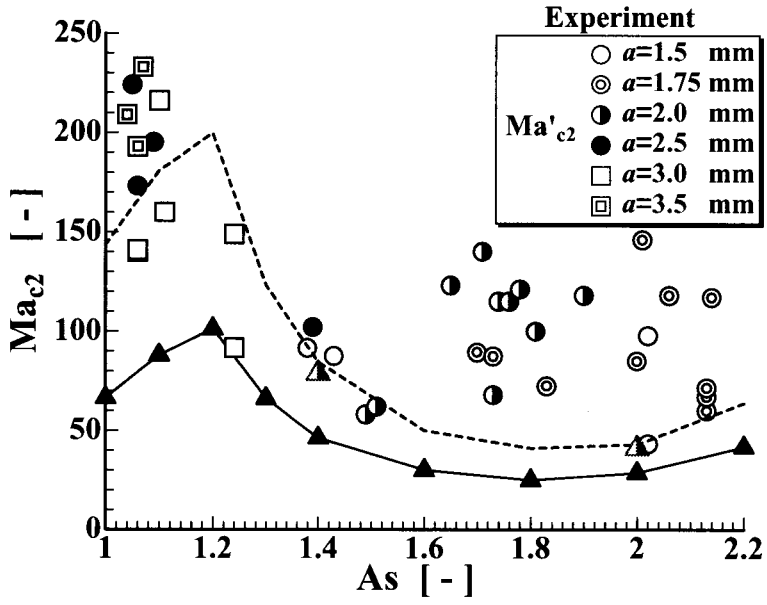

Fig.17 Ma_{c2} vs. As